Title

Optimal well placement and brine extraction for pressure management during CO2 sequestration

Authors

Cihan, Abdullah
Birkholzer, Jens T
Bianchi, Marco

Publication Date

2015-11-01

DOI

10.1016/j.ijggc.2015.07.025

Peer reviewed

Optimal well placement and brine extraction for pressure management during CO_2 sequestration

AbdullahCihan, Jens T.Birkholzer, MarcoBianchi[1]

Earth Sciences Division, Lawrence Berkeley National Laboratory, Berkeley, CA, USA

Available online 22 August 2015.

https://doi.org/10.1016/j.ijggc.2015.07.025

Highlights

- **This study presents a global optimization methodology for pressure management during geologic CO2 sequestration.**
- **A constrained differential evolution (CDE) algorithm is presented for well placement and injection/extraction rate control.**
- **The CDE method is demonstrated for a hypothetical CO2 storage scenario in a deep sandstone reservoir.**

Abstract

Large-scale pressure increases resulting from carbon dioxide (CO_2) injection in the subsurface can potentially impact caprock integrity, induce reactivation of critically stressed faults, and drive CO_2 or brine through conductive features into shallow groundwater. Pressure management involving the extraction of native fluids from storage formations can be used to reduce such pressure increases. However, dealing with large volumes of extracted brine can be technically challenging and expensive. Selection of optimal well locations and pumping rates are critical for maximizing CO_2 storage and minimizing brine extraction during geologic CO_2 sequestration (GCS). Robust and efficient computerized algorithms combining reservoir models and optimization methods are needed to make proper decisions on well placement and pumping rates. This study presents a constrained differential evolution (CDE) algorithm for solving global optimization problems involving pressure management of GCS projects. Application of the CDE optimization methodology was demonstrated for a hypothetical CO_2 storage scenario in a deep sandstone reservoir in the Southern San Joaquin Basin in California, USA. Industrial-scale storage of CO_2 would generate significant pressure buildup in this formation, which in turn would raise concerns about induced seismicity due to presence of multiple faults surrounding the injection site. Through the CDE optimization algorithm coupled to a vertically-averaged reservoir simulator, we successfully estimated optimal solutions for brine extraction wells in the reservoir that would limit the local pressure along the faults to a prescribed threshold. Multiple realizations of the reservoir permeability field were created to understand the impact of reservoir heterogeneity on optimization results. Our results indicate that the reservoir slope and heterogeneity have significant impact on optimum extraction rates. Reservoir heterogeneity is also a significant factor for extraction well locations, suggesting that in practice decisions about extraction well placement through optimization should be made at later project stages when data from a few years of

CO_2 injection have allowed iterative updating and refining of the reservoir forward models. Although the study focused on optimization of brine extraction, the CDE optimization methodology presented in this paper has also potential to solve other complex optimization problems related to GCS, such as increasing storage efficiency by enhancing injectivity and capillary and dissolution trapping.

1. Introduction

Injection of a large volume of CO_2 into deep geological reservoirs for geologic carbon sequestration (GCS) is expected to cause significant pressure perturbations in the subsurface (Nicot, 2008, Birkholzer et al., 2009). Large-scale pressure increases in injection reservoirs during GCS operations, if not controlled properly, may limit dynamic storage capacity and increase risk of environmental impacts (e.g., caprock damage, induced fault slippage, and leakage of brine and/or CO_2 into shallow fresh groundwater resources) (Birkholzer et al., 2012, Deng et al., 2012a, Deng et al., 2012b, Carroll et al., 2014). Thus, monitoring and controlling pressure buildup are critically important for environmentally safe and efficient implementation of GCS projects.

Extraction of native brine during GCS operations as a pressure management approach can increase storage capacity and reduce risk of environmental impacts (Court et al., 2011, Bergmo et al., 2011, Buscheck et al., 2011, Birkholzer et al., 2012). Extracted brine can be transferred to the surface for utilization or re-injected into overlying/underlying saline aquifers. However, brine extraction can be a significant factor in economic viability of a GCS project. Pumping, transportation, treatment and disposal of extracted brine can be challenging and costly (Harto and Veil, 2011, Harto et al., 2011, Middleton et al., 2012, Sullivan et al., 2013a, Sullivan et al., 2013b). Therefore, minimizing the volume of extracted brine, while maximizing CO_2storage and meeting other constraints needed for safe and efficient GCS operations, is an essential objective of the pressure management with brine extraction schemes.

To reduce the limitations of the brine extraction schemes with respect to the necessity of dealing with large volumes of extracted brine, in an earlier work (Birkholzer et al., 2012), the concept of “impact-driven pressure management (IDPM)” was introduced with the goal to limit pressure increases primarily where environmental impact is a concern, such as at a critically-stressed fault and/or a leaky well field. To design and optimize “impact-driven” pressure management options, Birkholzer et al. (2012) employed a derivative-based optimization methodology coupling the iTOUGH2 inverse-modeling framework (Finsterle, 2004, Finsterle and Zhang, 2011) and an analytical solution for single-phase flow in multilayered aquifer systems (Cihan et al., 2011). The optimization methodology was applied for brine extraction in response to a hypothetical injection scenario nearby a critically-stressed fault in a multilayered aquifer system. Time-dependent pumping rates from a series of extraction wells at fixed locations (either near to the injection zone or close to a fault) were computed to keep pressure buildup along the fault at or below a critical value for fault slippage, while minimizing the brine extraction ratio (brine extraction ratio is defined as ratio of total volume of extracted brine divided by the total volume of injected fluid.). The results from this study suggest that optimization of brine extraction can allow for a significant reduction in the brine extraction volumes needed to keep pressure increase in the storage formation below a given critical value. However, the placing of

injection and extraction wells is not intuitive in real cases because of heterogeneity in reservoir properties and complex reservoir geometry.

The brine extraction schemes coupled with CO_2 injection, which become particularly important for industrial-scale applications, must involve optimal well placement and control of injection/extraction rates in storage formations. Decisions on locations and operational rates of extraction wells can have substantial influence on total volume of extracted brine required to meet pressure buildup-related constraints. Non-optimal well placements and pumping rates can cause unnecessarily high extraction volume of brine and/or the pulling of CO_2 into brine extraction wells. Efficient computerized algorithms combining reservoir models and optimization methods are needed to make proper decisions on well locations and control parameters. In this study, optimization algorithms coupled with reservoir models are employed to minimize objective function (e.g., brine extraction ratio) by evaluating the outcome of reservoir models based on selections of well locations and injection/extraction rates.

Many applications involving reservoir models with optimization algorithms, both derivative-based and global algorithms, exist in the literature for solving practical subsurface problems related to hydrocarbon production (e.g., Guyagular et al., 2000, Yeten et al., 2003, Sarma and Chen, 2008, Wang et al., 2012), or groundwater production and groundwater remediation (e.g., Gorelick, 1983, Ahlfeld and Heidari, 1994, Maskey et al., 2002, Montoglou et al., 2004). Specifically for optimal well placement problems, due to complex reservoir geometry and heterogeneity in reservoir rock properties, objective functions tend to be highly irregular with multiple local optima in the parameter space (Bayer and Finkel, 2004, Humphries et al., 2013). Global optimization methods that involve derivative-free algorithms are generally preferred to solve optimization problems including optimal well placement. The derivative-based optimization algorithms (e.g., gradient projection method, sequential quadratic programming) are generally used for optimal rate control parameters of wells, resulting in smooth and continuous objective functions (Montoglou et al., 2004, Bellout et al., 2012), although examples of using derivative-based methods with numerical reservoir models also exist in the literature for optimal well placement problems (e.g., Zandvliet et al., 2008, Zhang et al., 2010). The irregularity of objective functions due to complex reservoir heterogeneity and geometry can easily cause derivative-based method solutions to be stuck in a local minimum. In addition to that, the discrete nature of grid-based numerical models for well locations and the presence of complex well control parameters (time-dependent functions with multiple parameters for injection/extraction/bottom-hole pressure control) make the derivative-free global optimization methods more suitable for solving the coupled optimal well placement and rate control problems in application to GCS. However, global optimization methods such as commonly used evolutionary algorithms require a large number of forward model runs to reach a global optimum. As a result parallelization of the algorithms in the multi-processor computer or cluster environment is typically needed for solving larger reservoir problems in a computationally efficient manner (Guyagular et al., 2000, Bellout et al., 2012).

This study, built upon our earlier work in Birkholzer et al. (2012), presents a global optimization methodology for pressure management during geologic CO_2 sequestration. A modified differential evolution (DE) algorithm is introduced for solving constrained global optimization problems involving well placement and brine extraction to control pressure increases during GCS. DE is a parallel direct

search method that was originally developed by Storn and Price (1995) and has been proven to be a very powerful evolutionary algorithm (Storn and Price, 1996) with good convergence properties, simplicity of use and understanding, and suitability for parallelization. Since the DE's first development, different variants have been proposed for accelerating its convergence rate (Price et al., 2005), but the original method is in general applicable to unconstrained optimization problems. In this work, we have modified the DE algorithm based on Deb (2000) to solve constrained global optimization problems relevant to GCS projects.

In the following, first a formal description of the optimization problem is given focusing on brine extraction for pressure management during GCS. Then, the constrained differential evolution (CDE) methodology is described and tested for a simple optimization problem whose optimal solution can be found with other optimization methods. Finally, a more realistic application of the global optimization methodology is presented for CO_2 injection scenarios in the Vedder Formation in the Southern San Joaquin Basin in California, USA. Optimal placements of wells and selection of brine pumping rates are evaluated for different realizations of reservoir heterogeneity subject to maximum pressure buildup along the faults. Well locations and rates are also optimized under the constraint that no CO_2 is to be pulled into extraction wells. A numerical vertically averaged two-phase flow simulator is employed as the forward model for the optimization calculations with the CDE.

2. Problem description

The focus in this paper is on optimization of brine extraction for controlling pressure locally in environmental impact zones (e.g., faults, leaky abandoned well fields). Let the total volume of injected CO_2 be denoted by V_{inj} and the total volume of extracted fluid by V_{ext}. The goal is to minimize the extraction ratio defined by V_{ext}/V_{inj}. The optimization problem involving the objective function and the constraints, respectively, can be formally expressed as

$$\text{Minimize} f(\boldsymbol{p}) = \frac{V_{ext}}{V_{inj}} \tag{1}$$

$$\begin{aligned} \text{Subject to} \quad & g_1(\boldsymbol{p}) = V_{ext,CO_2} = 0 \\ & g_2(\boldsymbol{p}) = \Delta \boldsymbol{p}_{crt} - \max\{\Delta P(\boldsymbol{x}_{obs}, \boldsymbol{y}_{obs}, t)\} > 0 \end{aligned} \tag{2}$$

where $\boldsymbol{p}$ is the parameter vector that may include locations of injection wells (x_{inj}, y_{inj}) and extraction wells (x_{ext}, y_{ext}), and constant or time-dependent function parameters for controlling injection and extraction. Specific costs associated with the pumping per volume of injected or produced fluid and treatment of extracted brine are assumed to be proportional to the extraction ratio defined in Eq. (1). Other costs related to drilling of wells are not considered.

The first constraint in Eq. (2) imposes that no CO_2 breakthrough will occur at the extraction wells to secure for all the injected CO_2 to remain in the reservoir. The second constraint represents the pressure management goal of keeping reservoir pressure increases in defined impact zones below one (or more) critical pressure buildup values (ΔP_{crt}) (with respect to the pressure prior to the injection). We may assume that an environmental impact can be expected if the pressure buildup at any location in the impact zones exceeds ΔP_{crt}. Pressure buildup at impact zones is recorded through

a vector of observation points (x_{obs}, y_{obs}), as many as required. Denoting the number of injection wells by N_{inj} and the number of extraction wells by N_{ext}, the total injected volume of CO_2 and the total extracted volumes of brine and CO_2 can be expressed by

(3)Vinj=∑i=1Ninj∫0∞Qinj,CO2xinj,yinj,i,tdt

$$V_{\text{inj}} = \sum_{i=1}^{N_{\text{inj}}} \int_0^{\infty} Q_{\text{inj},\text{CO}_2}(x_{\text{inj}}, y_{\text{inj},i}, t)\mathrm{d}t \tag{3}$$

$$V_{\text{ext}} = V_{\text{ext},b} + V_{\text{ext},\text{CO}_2} = \sum_{i=1}^{N_{\text{inj}}} \int_0^{\infty} [Q_{\text{ext},b}(x_{\text{ext},i}, y_{\text{ext},i}, t) + Q_{\text{ext},\text{CO}_2}(x_{\text{ext},i}, y_{\text{ext},i}, t)]\mathrm{d}t \tag{4}$$

The optimization problem also involves parameter bounds as additional constraints, which are not shown in Eq. (2). Specific bounds on parameters will be discussed in Sections 2 Problem description, 3 Global optimization methodology when applying the optimization methodology to example optimization problems.

For the applications in this paper, we considered only vertical and fully penetrating wells for the injection and the extraction in the storage reservoir, and we also assumed that an injection well has a fixed known location. However, we have defined the optimization problem and its CDE solution in a general manner such that applications including the well placement problems for injection wells or other well shapes and properties can be easily accommodated. For applications involving horizontal, tilted or partially penetrating wells, additional parameters such as orientation, depth and screened length of the wells can be included into the optimization problem as unknowns (e.g., Yeten et al., 2003).

Although not discussed in this paper, the CDE optimization methodology introduced in the next section can also solve other specific optimization problems such as enhancing injectivity and storage efficiency (e.g., Zhang and Agarwal, 2013, Shamshiri and Jafarpour, 2012). However, the CDE method (any other evolutionary and stochastic algorithm), which tend to require a large number of forward model runs to find the global minimum, requires selection of computationally efficient models. Thus a balance is needed to keep higher computational efficiency while representing the physics of the problem reasonably well by a forward model with sufficient fidelity.

3. Global optimization methodology

In this section, the basic strategies of the DE algorithm (Storn and Price, 1997) and modifications to obtain CDE for treatment of constraints are described. Then, the CDE is tested for a simple pressure management problem.

3.1. Constrained differential evolution (CDE) algorithm

A DE algorithm has four main steps consisting of initialization, mutation, crossover and selection (Storn and Price, 1997). Initialization involves generation of NP D-dimensional parameter vectors. The dimension D is equal to the number of unknown parameters, and each parameter vector

represents one member of a NP-sized population. The number of members, NP, stays fixed during the optimization process. Parameters of the vectors at the initial generation can be selected randomly from the entire parameter space based on user-defined parameter bounds and/or prior knowledge, if available. Let the NP *D*-dimensional parameter vectors be denoted as

$$\boldsymbol{p}_i^G; i = 1,2,\ldots,\mathrm{NP} \tag{5}$$

where *G* is the generation (or iteration) number, and *G* is equal to 0 at the initial generation step. At each new generation step *G* + 1, DE produces an intermediary population containing mutant vectors for each member of $\boldsymbol{p}_i$(referred to as target vector). The basic DE strategy constructs new parameter vectors (mutant vectors) by adding weighted differences of two population vectors to a third vector. This step is called mutation. Since the first development of the basic strategy, many different mutation strategies have been devised and used for different types of optimization problems (Price et al., 2005). In this study, a variant of the basic mutation strategy based on linear combination of the best member ($\boldsymbol{p}_{\mathrm{best}}^G$, the vector giving the best objective function value) and current members of the population at *G* has been selected because of its higher computational efficiency for the problems tested in this manuscript. For each target vector $\boldsymbol{p}_i$ (*i* = 1,…,NP), a mutant vector $\boldsymbol{v}_i$ is produced by

$$\boldsymbol{v}_i^{G+1} = \boldsymbol{p}_i^G + F_c(\boldsymbol{p}_{\mathrm{best}}^G - \boldsymbol{p}_i^G) + F_m\left(\boldsymbol{p}_{r1}^G - \boldsymbol{p}_{r2}^G\right); i = 1,2,\ldots,\mathrm{NP} \tag{6}$$

where r_1 and r_2 are random mutually different integers ∈{1,2, …,NP}, selected to be different from the index *i*. F_c is the random combined factor ∈[0,1] that controls the magnitude of the contribution of the differential variation ($\boldsymbol{p}_{\mathrm{best}}^G - \boldsymbol{p}_i^G$), and F_m is the random mutation scaling factor ∈[−1,1] that controls the magnitude of the contribution of the differential variation ($\boldsymbol{p}_{r1}^G - \boldsymbol{p}_{r2}^G$). Then, parameters of the mutant vectors ($v_{i,j}^{G+1}$, *j* = 1,…,D) are combined with the parameters of the target vector ($p_{i,j}^G$, *j* = 1, …,D). This is called crossover operation, and the resultant vectors are trial vectors, $\boldsymbol{u}_i^{G+1} = (u_{i,1}^{G+1}, u_{i,2}^{G+1}, \ldots, u_{i,D}^{G+1})$, which are formed by

$$u_{i,1}^{G+1} = \left\{ \begin{array}{ll} v_{i,j}^{G+1} & \mathrm{if}(\omega \le \mathrm{CR}) \\ p_{i,j}^G & \mathrm{otherwise} \end{array} \right\}; j = 1,\ldots,\mathrm{D}; i = 1,\ldots,\mathrm{NP} \tag{7}$$

where *ω* is a random real number ∈[0,1] generated from the uniform distribution, and CR is the crossover factor that is a user-specified constant ∈[0,1]. The parameters of the trial vectors (Eq. (7)) are not allowed to extend beyond their maximum and minimum values to satisfy the constraints on parameter bounds.

The last step in the DE algorithm is the selection process for the surviving members of the population. In this step, the objective function values of the trial vector, obtained by running the forward model for each population member, are compared to those of the target vector. The trial vectors giving smaller objective functions replace the corresponding target vectors, and otherwise the old values are kept. The selection of new target vectors can be represented as

$$p_{i,j}^{G+1} = \begin{cases} u_{i,j}^{G+1} & f_i(u_{i,j}^{G+1}) \le f_i(p_{i,j}^{G}) \\ p_{i,j}^{G} & \text{otherwise} \end{cases}; j = 1, \ldots, \mathrm{D}; i = 1, \ldots, \mathrm{NP} \quad (8)$$

In this work, the selection process of the DE algorithm, specifically the comparison of the trial vectors with the target vectors, is modified to take into account constraints. We refer to this modified algorithm as constrained differential algorithm, or CDE. Deb (2000) proposed a general constraint handling methodology for evolutionary algorithms. A term, as a function of constraint violation magnitude, is added to the objective function to penalize infeasible solutions (violating constraints in Eq. (2)), but different from conventional penalty function methods, no penalty terms are needed for constraints. Deb (2000) proposed a tournament selection operator based on the following criteria: (1) Any feasible solution is preferred to any infeasible solution, (2) among two feasible solutions, the one having the smaller objective function value is preferred, and (3) among two infeasible solutions, the one with the smaller constraint violation is preferred. Following Deb (2000), objective functions of the trial vectors satisfying these criteria can be expressed as

$$f_i\left(u_{i,j}^{G+1}\right) = \begin{cases} f_i\left(u_{i,j}^{G+1}\right) & g_{i,k}(u_{i,j}^{G+1}) \ge 0 \forall k = 1,2,\ldots,M \\ f_{\max}\left(p_{i,j}^{G}\right) + \sum_{k=1}^{M} \left| g_{i,k}(u_{i,j}^{G+1}) \right| & \text{otherwise} \end{cases} \quad (9)$$

where M is the total number of constraints, f_{max} is the worst objective function value among the feasible solutions of the population at generation G, and $g_{i,k}$ is the value of the kth constraint violation for population member (or parameter vector) i. All the constraints are typically normalized to avoid bias among different constraints. Eq. (9) specifies that the objective function resulting from an infeasible solution depends on the magnitude of the constraint violations and the maximum objective function value of the feasible solutions in the population, while the objective function of a feasible solution is equal to the its objective function value. By use of Eq. (9) into Eq. (8), new target vectors are selected. Compared to DE, CDE requires evaluations and storage of not only the objective functions but also of the constraints by running the forward model for NP parameter vectors at each new generation. The general steps of the CDE algorithm can be listed as follows:

1. Generate NP parameter vectors (randomly and/or user-defined) and compute objective functions and constraints $f_i(\boldsymbol{p}_i^0)$ and $g_{i,k}(\boldsymbol{p}_i^0)$, respectively, to identify feasible and infeasible members (parameter vectors) in the initial population ($G \leftarrow 0$),
2. Determine the best and the worst feasible objective functions with the associated vectors in the initial population,
3. Set the generation (or iteration) number $G \leftarrow G + 1$, and generate NP mutant vectors from the target vectors at the previous generation by using Eq. (6),
4. Conduct crossover operation and generate trial vectors using Eq. (7),

5. Evaluate objective functions and constraints (by running the forward model) for each trial vector (Eq. (9)),
6. Select the new parameter target vectors (Eq. (8)),
7. Determine the best and the worst objective functions of the feasible solutions in the new population, and check the tolerances. If the tolerances specified (and other possible termination options) are met, then terminate, or else return to step 3.

Price et al. (2005) discussed several termination options that can be selected based on the specific nature of an optimization problem. For the examples in this manuscript, termination occurs if the difference between the best and the worst value of the population becomes less than a predetermined tolerance, which was set to 10^{-5}. A limit on the maximum number of iterations was also employed; 200 iterations were sufficient to reach the tolerance in all the example cases.

Proper selection of control parameters (NP, F_m, F_c, CR) is critical to prevent premature convergence, stagnation, or slow rate of convergence. Storn and Price (1997) state that reasonable values for NP lie between 5 × D and 10 × D. Later experiences show that optimum values of parameters depend on the mutation strategy (e.g. Eq. (6)) and can vary for different problems (Price et al., 2005). In our applications, we always selected NP ≥ 5 × D to obtain sufficient diversity in population members to reduce risk of premature convergence. Zaharie (2002) showed that premature convergence can be prevented if the mutation and crossover factors induce an increase of the population variance. Results from Rudolph (1996) on convergence of evolutionary strategies state that if the mutation operator has a random character and the selection process is elitist (the best-so-far solution is always retained), then the algorithm converges to a global optimum in the long term. Therefore, randomization of the mutation scaling factor and the combined factor in Eq. (6) is expected to be a sufficient (but not necessary) condition for the convergence of the algorithm. Selection of a high value for CR close to 1 (e.g., 0.9) has been seen to speed up the convergence of the algorithm for some problems, while too high a value in some cases might increase the risk of premature convergence (Storn and Price, 1997, Price et al., 2005). A further discussion on the selection of CR will be given in the next section when applying the algorithm to a test problem.

We implemented the CDE algorithm described above by modifying an existing FORTRAN90 code for DE algorithm developed by Dr. Feng-Sheng Wang and his students (http://www1.icsi.berkeley.edu/~storn/code.html#f90c). The modified code was parallelized for running multiple forward model simulations simultaneously in multi-processor computing environments.

3.2. Testing of the CDE algorithm for a simple pressure management problem

The performance of the CDE algorithm is tested for a simple optimization problem involving placement of a brine extraction well and optimization of the extraction rate. The test problem is defined such that the optimal extraction location is in fact known and that a derivative-based optimization method can be used to determine the extraction rate. An injection well placed at the origin injects fluids at a constant rate of 1.67×10^4 m^3/d for 50 yr into a 60 m-thick aquifer overlaid by a 100 m-thick aquitard. The aquifer has a permeability of 3.0×10^{-13} m^2 and a specific storativity of 1.69×10^{-6} m^{-1}. The aquitard has a permeability of 10^{-18} m^2 and a specific storativity of 1.98×10^{-6} m^{-1}.

Two abandoned wells exist (red colored) at 20 km east and south of the injection well (Fig. 1), and they are assumed to have the potential to leak and transmit poor-quality water into a freshwater aquifer above the aquitard. The critical pressure buildup (ΔP_{crt}) for brine leakage to occur into the freshwater aquifer through the potentially leaky abandoned wells is assumed to be 0.2 MPa.

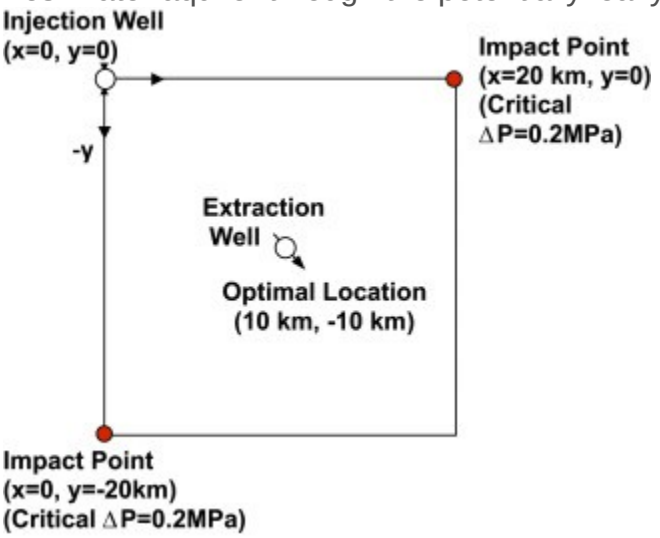

Download high-res image (154KB)

Download full-size image

Fig. 1. Example optimization problem for testing the CDE optimization method.

The goal is to use an extraction well, operating with a minimum extraction ratio (V_{ext}/V_{inj}), to keep the pressure buildup below the critical pressure buildup at the abandoned well locations for preventing any possible leakage. In this example, a single-phase analytical model (Cihan et al., 2011) is selected as the forward model to simulate pressure buildup in the layered aquifer system in response to injection and extraction. Since single-phase flow conditions are assumed, the minimization problem contains only the second constraint in Eq. (2), in addition to other constraints on parameter bounds. The optimal extraction well location is known to be at (x = 10 km, y = −10 km) because of symmetry considerations, but the optimal rate is not known and can vary as a function of time. We tested two extraction scenarios; in the first case, the extraction rate is assumed to be constant during the duration of the injection, whereas in the second case, the extraction is assumed to occur over six predefined time periods with varying uniform rates for each period. Since the location of the extraction well is known, a derivative-based algorithm can easily be implemented to find optimal extraction rates. The CDE algorithm is applied to estimate both optimal extraction rate(s) and optimal well location. Then, the results of the CDE algorithm are compared to the known well location, and to the extraction rate results obtained from a derivative-based optimization method, using a sequential quadratic programing (SQP) algorithm built into the Fortran IMSL library. We use the SQP algorithm that was developed by Spellucci (1998) for nonlinear optimization problems with equality and inequality constraints to estimate optimal extraction rate(s) with known well locations.
For the first extraction scenario, the number of unknown parameters for the CDE is equal to 3 (D = 3). The isosurface line in Fig. 2 separates the feasible from the infeasible zones for the parameter

vectors. Each circle represents a 3-dimensional parameter vector or a member of the population. The parameter vectors were generated randomly at iteration = 0 based on a uniform distribution for a predefined range of parameter values (i.e., for the 3D problem, $x \in [0,20\ \text{km}]$, $y \in [-20\ \text{km}, 0]$, and $Q_{ext} \in [-Q_{inj}, 0]$). The population members that fall below the isosurface line are in the infeasible zone. Fig. 2a–d demonstrate that the infeasible members of the population transfer to the feasible zone as the iterations increases, and finally converge to the optimal parameter vector for the location (x, y) and the normalized extraction rate, $Q_{ext}/(-Q_{inj})$ (i.e., the uniform extraction rate divided by the injection rate for single time-period extraction).

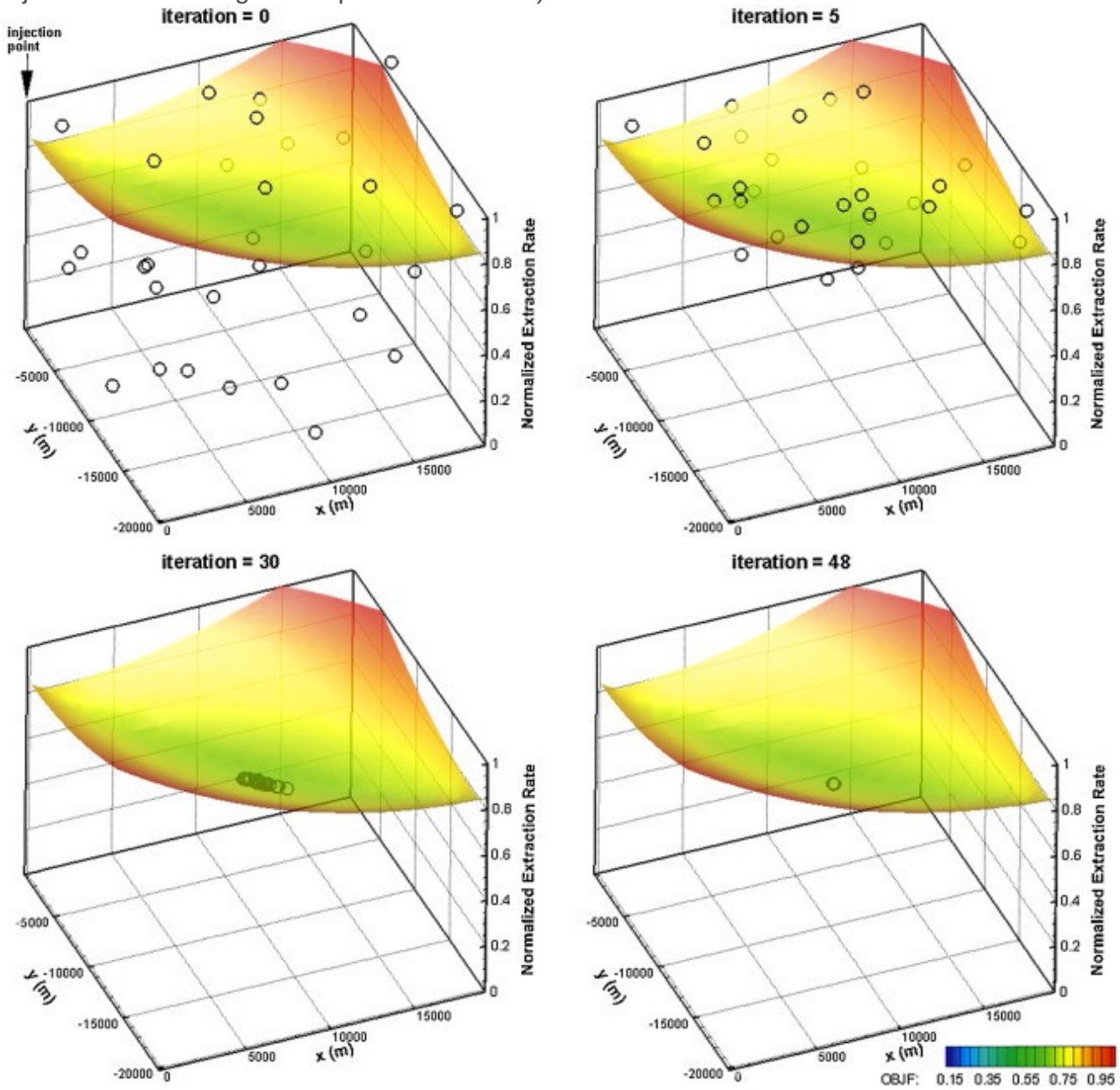

Download high-res image (1MB)

Download full-size image

Fig. 2. Demonstration of the CDE optimization algorithm on a simple test problem, the zones below the isosurface line are infeasible.

There is no exact way of testing truthfulness of the optimal brine extraction ratio calculation for complex problems as the actual optimum is not known. However, multiple optimization runs with different optimization strategies or parameter sets are useful to test consistency of the results. Fig. 3 shows the effect of the mutation scaling factor (CR), which is the only fixed parameter in addition to NP, on evolution of the objective function for the 3D problem as a function of the number of objective function evaluations (or forward model runs). As the CR values increase, the rate of decrease in the objective function appears to be faster. The algorithm was run for a long time by selecting a very tight termination criterion based on the difference between the best and the worst population members. From Fig. 3, it can be concluded that the optimization with CR = 0.9 reaches an acceptable minimum value of the objective function in less than 500 forward model runs, while the optimization with CR = 0.5 takes about three times longer. However, higher values of CR than 0.9 result in stagnation, where the objective function decreases extremely slowly, and the algorithm does not reach the global minimum at the maximum specified number of iterations. Based on these results, we select a CR value of 0.8 in all the optimization calculations in this manuscript in order to obtain the optimization results more efficiently with less risk of stagnation or premature convergence.

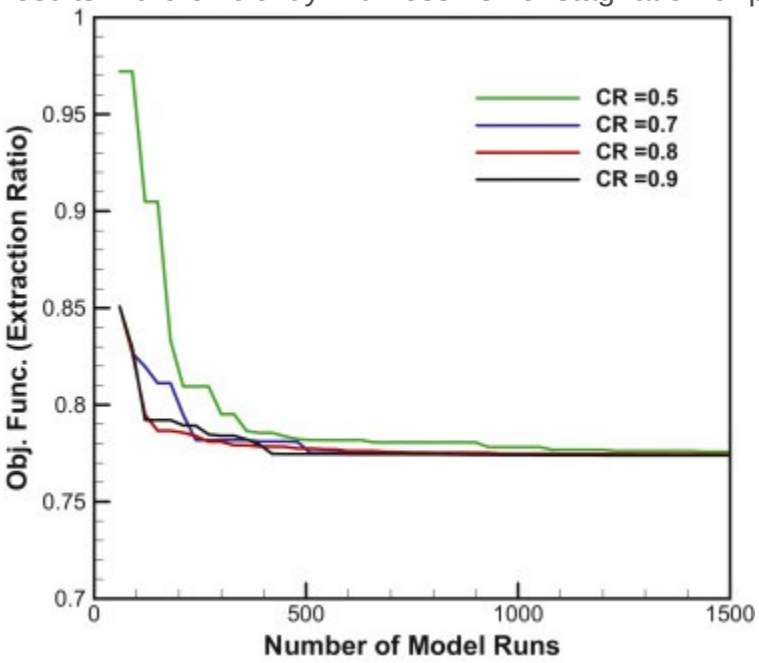

Download high-res image (182KB)

Download full-size image

Fig. 3. Effect of DE optimization parameter, crossover factor (CR), on evolution of objective function as a function of number of model runs or number of objective function evaluations.

As shown in Table 1, the CDE search finds the optimum well location, and the extraction rates obtained by CDE agree very well with those calculated by the SQP method for both the 3D problem and the 7D problem. NP was selected as $10 \times D$ in both cases. Dimension or number of unknowns for the problems solved by the SQP is two parameters less than the CDE because the SQP method does not solve for the extraction well location. The table also compares the number of objective function evaluations during optimization by the CDE and the SQP algorithms. Although the larger number of

forward models required for the CDE may seem to be an issue for very large numerical forward models, the CDE algorithm is easily parallelizable, which allows for very fast computation in a multi-processor computer or cluster environment. For instance, the total process time of the optimization with the serially implemented SQP algorithm was comparable to that with the CDE algorithm, which was implemented with OpenMP using 5 processors in a desktop workstation (Dell Precision T3600 Intel Xeon 3.6 GHz).

Table 1. Optimization results for the simple test problem.

	CDE (D = 3)	**SQP (D = 1)**		**CDE (D = 7)**	**SQP (D = 5)**
x (km)	10.070	–	x (km)	10.050	–
y (km)	−10.070	–	y (km)	−10.050	–
Q (m^3/d)	-1.049×10^4	-1.049×10^4	Q_1 (m^3/d)	-9.063×10^2	-9.141×10^2
Optimal Ext. ratio	0.774	0.774	Q_2 (m^3/d)	-9.190×10^3	-9.190×10^3
Number of Obj. Func. evaluations	1620	12	Q_3 (m^3/d)	-1.024×10^4	-1.024×10^4
			Q_4 (m^3/d)	-1.199×10^4	-1.196×10^4
			Q_5 (m^3/d)	-3.319×10^2	-4.060×10^2
			Optimal Ext. ratio	0.620	0.621
			Number of Obj. Func. evaluations	22,000	2366

Comparing the calculated extraction ratios for the 3D and 7D problems, we can conclude that selecting multiple extraction rates or a time-dependent extraction rate function can notably help reduce the total volume of extracted brine. Another interesting result from this simple test is that the optimal well location estimated by the CDE stays the same irrespective of the form of the extraction rate function. This indicates for the simple problem tested (with a symmetric layout) in this section that the well placement optimization problem can be uncoupled from the rate optimization problem. If uncoupling of these two problems is indeed possible, the computational efficiency could be increased because the global methods can be used to find the optimal well placements (with reduced number of parameters) while derivative-based methods that are more efficient than the global methods can be used to solve well control or rate optimization problems. However, this is not necessarily always the case; especially for more complicated problems as in the example in Section 4, including heterogeneous reservoir properties, faults and risk of CO_2 breakthrough, uncoupling may not guarantee the actual optimal solution.

4. Application of the CDE optimization method for a realistic CO_2injection scenario

In this section, we test the applicability of the CDE algorithm for a CO_2injection scenario in a large-scale realistic geological setting. We selected the Vedder Formation in the Southern San Joaquin Basin in California, USA. Hydrogeological properties are known based on site characterization data available from oil and gas exploration and groundwater development in the area (USGS, 2007, Wainwright et al., 2013). The Vedder Formation is quite permeable providing for sufficient

injectivity, and the overlying Temblor–Freeman Shale is considered a suitable caprock for stratigraphic containment of the injected supercritical CO_2. The site has challenging stratigraphic and structural complexity, caused by the existence of numerous faults, and there is concern about reservoir compartmentalization and pressure-induced seismicity. The Vedder Formation has been used in the past to evaluate pressure impacts for a hypothetical storage scenario with injection of 5 Mt CO_2/yr over 50 years (e.g., Birkholzer et al., 2011). The site has also been used for risk assessment, sensitivity and uncertainty quantification studies (e.g., Wainwright et al., 2013, Pawar et al., 2014).

One important result from the earlier simulation studies is that the two faults on the east and west of the injection site (Fig. 4) will experience significant pressure buildup during and after injection. Concerns about induced seismicity would almost certainly require pressure management at this site, and pressure management via targeted brine extraction seems particularly suitable because the pressure control needs to be along the faults. On the other hand, well locations and pumping rates need to be carefully designed to minimize extraction volumes and to avoid pulling CO_2 into the extraction wells and even near the faults.

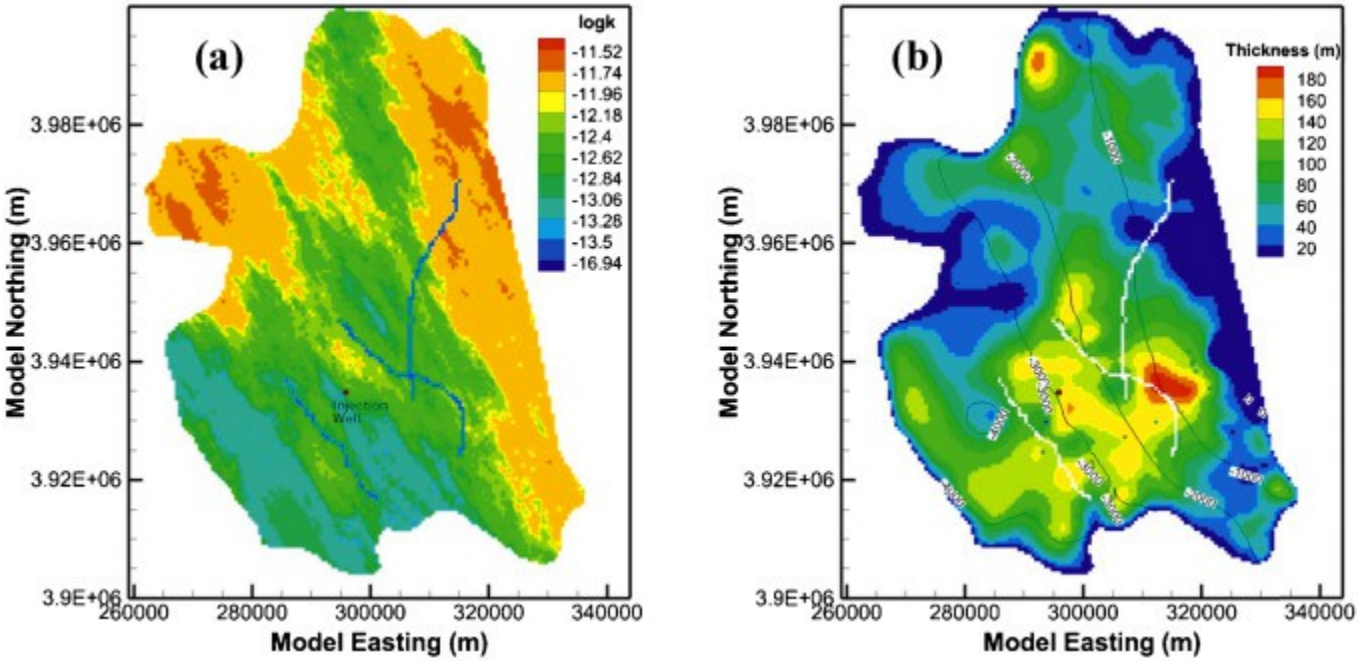

Download high-res image (739KB)

Download full-size image

Fig. 4. (a) A realization of the heterogeneous permeability field of the top Vedder Sand Formation. The map also shows faults (dark blue) considered in the model and the injection well. (b) Contour plots for the thickness and the top elevation (black lines) of the first Vedder Sand. (For interpretation of the references to color in this figure legend, the reader is referred to the web version of this article.)

4.1. Numerical reservoir model

The Vedder Formation involves six alternating sand/shale layers. The thickest sand layer (the first Vedder Sand) with a maximum thickness of 197 m is located at the top portion underlying the Temblor-Freeman shale. We considered only the first Vedder Sand to model the hypothetical

CO_2 storage and to apply the CDE algorithm for pressure management with brine extraction. Fig. 4 shows the injection well location and the contour maps of the first Vedder Sand thickness and the top elevation (above sea level). As in Wainwright et al. (2013), we considered only the three major faults fully penetrating the Vedder Sand. The faults are likely sealing faults and in this study are represented as linear features with two orders of magnitude lower permeability than the Vedder Sand. The Vedder Sand outcrops toward the eastern boundary. Along the northern, western, and southern boundaries, the Vedder Sand pinches out into the shale and becomes thin or absent along these boundaries. Thus, the western, northern and southern boundaries are no flow boundaries, and the eastern boundary is set to a fixed pressure boundary. For simplicity, the reservoir top and bottom boundaries are also no flow boundaries. Not allowing pressure diffusion and preventing slow brine flow into the caprock in response to the injection is a conservative assumption in terms of reservoir pressure buildup, and therefore the pressure buildup estimations based on this model are higher than those assuming very low caprock permeability in preceding simulation studies (Birkholzer et al., 2011, Wainwright et al., 2013).

Porosity, permeability, two-phase flow parameters (Table 2) and initial conditions are based on the earlier studies about this site (Zhou and Birkholzer, 2011, Birkholzer et al., 2011, Wainwright et al., 2013). Initially hydrostatic conditions (based on pressure, temperature and salinity data) are assumed, and the fluids are also assumed to be incompressible with densities of 989 kg/m^3 for brine and 819 kg/m^3 for $scCO_2$. We considered only horizontal heterogeneity in this study based on the average horizontal permeability data available from existing wells in the vicinity of the site. A sequential Gaussian simulation by the SGSIM code of the Geostatistical Software Library (GSLIB) (Deutsch and Journel, 1998) was utilized to generate the conditional realizations of log (k) (permeability) fields. The random realizations were conditioned to 16 permeability measurement points, and the resolution of the model domain in the x- and y-directions was selected to be Δx = 562.6 m and Δy = 565.9 m. The generated random realizations serve only for demonstrating an application of the optimization methodology and understanding heterogeneity effects on optimization results, rather than modeling the actual Vedder Sand reservoir geology. Porosity was distributed in the numerical model domain according to a logarithmic relationship between porosity (ϕ) and permeability. The porosity-permeability relationship, fitted based on the available data from the site, can be expressed as $\phi = 0.0438 \times \ln(k) + 1.4915$ ($R^2 = 0.76$). A locally heterogeneous two-phase flow model parameter α (i.e., equivalent to the inverse of the entry capillary pressure for CO_2 into the reservoir rock) was assigned into the model by the Leverett scaling approach (Leverett, 1941] $\left(\alpha \sim \sqrt{k/\phi}\right)$, where we used the local averages (from Table 1) to scale $\alpha$for the heterogeneously distributed values of porosity and permeability in the numerical model domain.

Table 2. Assumed average values of the two-phase flow properties in the Vedder Sand.

Properties	Local average values
Porosity	0.264
Permeability (m^2)	2.990×10^{-13}

Properties	Local average values
Pore Compressibility (Pa^{-1})	4.900×10^{-10}
*α (m^{-1})	1.263
*n	1.842
+S_{rw}	0.300
+S_{rn}	0.200

*α, n: van Genuchten model parameters (1980).

+S_{rw}, S_{rn}: residual saturations for wetting (brine) and nonwetting (CO_2) fluids.

We employed a numerical vertically-averaged two-phase flow model for representing CO_2/brine flow in the first Vedder Sand. This modeling approach has been known and used for a long time in petroleum reservoir engineering (Coats et al., 1971), non-aqueous phase liquid migration in application to groundwater contamination (Parker and Lenhard, 1989, Wu et al., 1994) and more recently CO_2 /brine flow in the context of GCS (Nordbotten et al., 2005, Dentz and Tartakovsky, 2009, Juanes et al., 2010, Gasda et al., 2012). Such models are based on vertical integration of the 3D two-phase flow equations under the assumption of vertical equilibrium (VE) or hydrostatic pressure distribution in each phase. Once the assumption of vertical equilibrium behavior is appropriate for a particular reservoir, the vertically-averaged models become very advantageous over the full 3D models especially for large-scale reservoir modeling and optimization studies because they are computationally much more efficient with reduced dimensionality. Earlier studies (e.g., Court et al., 2012, Guo et al., 2014) indicate that the VE can be a good approximation for GCS applications with very large temporal scales and large horizontal extent (compared to the thickness of the reservoir) in relatively high permeability (e.g., $\geq 10^{-13}$ m^2) and vertically homogeneous reservoirs. The numerical model of the first Vedder Sand was represented by a quasi-2D mesh (i.e., 2D mesh with varying thickness). We selected the same numerical model resolution (Fig. 4a) as the generated geostatistical model of permeability distribution. In such a large domain with a very local CO_2injection, solution of two partial differential equations for the whole domain is not necessary, as the two-phase conditions will prevail only in a small portion of the domain. In order to make the numerical model even more efficient, the two-phase flow equations (two partial differential equations) were solved only in a rectangular zone around the injection point that is large enough (~15 km × 15 km used) so that the injected CO_2 would not reach the boundary of this zone during a long simulation time (~100 yr). Beyond the predefined zone, only one partial differential equation for single-phase flow of brine needs to be solved.

4.2. Optimization for well placement and extraction rate control

Following earlier works, we assumed a hypothetical storage scenario of 5 Mt CO_2 injected per year at a constant rate for 50 years. When there is no pressure control via brine extraction, the numerical simulations were conducted a priori to evaluate pressure buildup and CO_2 plume distribution for each realization. In Fig. 5a, the pressure buildup contour lines at the end of injection are superimposed on

the permeability map for Realization 1. Fig. 5b shows for the same realization the average CO_2 saturation map and the reservoir top elevation contour lines. The plume migration appears to be controlled mainly by the slope of the reservoir top elevation, as the buoyancy forces direct the CO_2 plume along the direction of the increasing elevation. Heterogeneity in reservoir properties has also some effect on the plume shape, but its impact on the pressure buildup seems more important. The peak value of the maximum pressure buildup along the faults ranges from about 1.5 MPa for Realization 3 to about 2.7 MPa for Realization 1 (Fig. 8a). In this study we assumed a threshold value of 1 MPa as the maximum pressure buildup that can be sustained without activating the faults. We first conducted basic optimization studies with the SQP algorithm without brine extraction to calculate the maximum possible constant injection rate for each realization that does not violate the 1 MPa pressure buildup constraint along the faults. The maximum allowed constant injection rates without brine extraction appear to be about 35% to 65% less compared to the goal of a 5 Mt/yr injection rate (Table 3). Second, we conducted an optimization of brine extraction (well locations and rates) to be able to inject 5 Mt of CO_2 over 50 years without violating the 1 MPa pressure threshold along the faults, with the additional goals of extracting as little brine as possible and not pulling any CO_2 into the extraction wells.

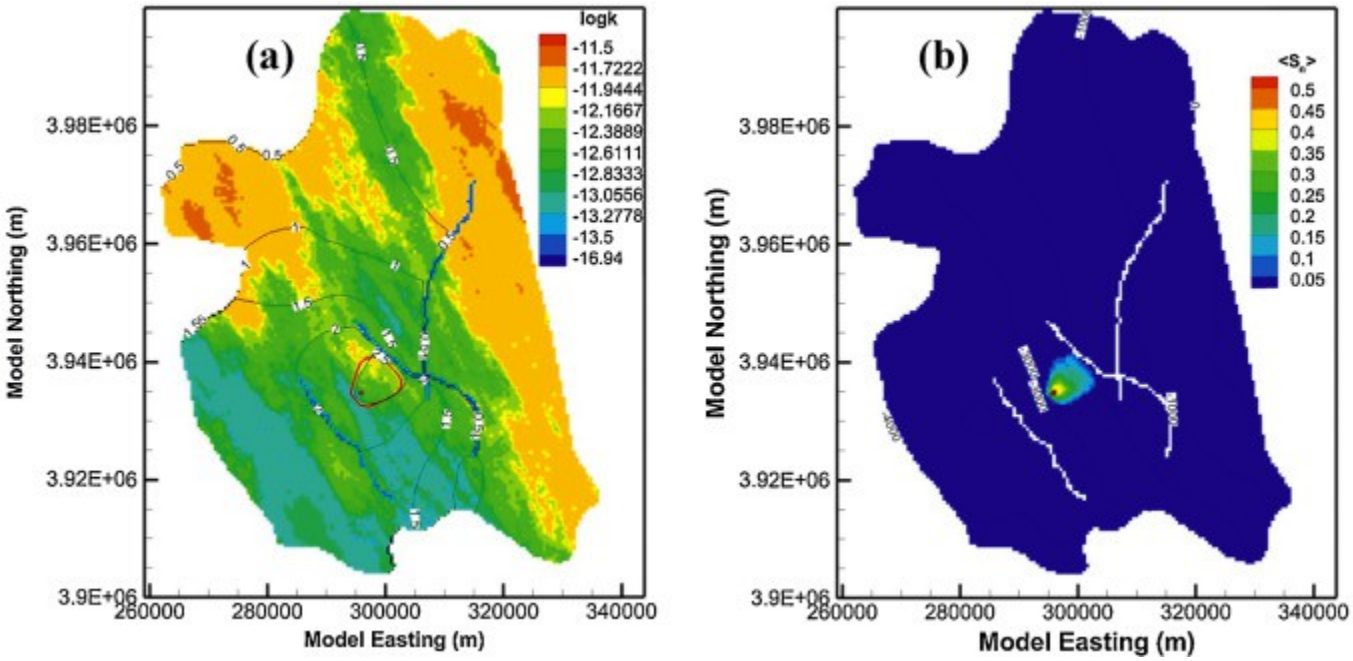

Download high-res image (615KB)

Download full-size image

Fig. 5. (a) Pressure buildup contour lines (in MPa) at the end of 50 years without brine extraction superimposed on the permeability (in log 10) map of Realization 1. (b) Saturation contour plot overlaid with the contour lines of the top reservoir elevation.

Table 3. Optimal injection rates without brine extraction.

Realization	Optimal injection rates without brine extraction for ΔP_{max} = 1 MPa
1	1.968 Mt/yr
2	2.739 Mt/yr

Realization	Optimal injection rates without brine extraction for ΔP_{max} = 1 MPa
3	3.229 Mt/yr
4	2.061 Mt/yr
5	2.451 Mt/yr

As a reminder, the objective function in this example is to minimize the extraction ratio (Eq. (1)), subject to the constraints given by Eq. (2). Optimal placement of wells and selection of time-dependent brine pumping rates were evaluated for five different realizations. Two brine extraction wells are initially assigned and assumed to operate with different time-dependent extraction rate functions. However, during the optimization runs, the wells are allowed to occupy the same numerical grid block or to have zero brine production. Our earlier pressure management and optimization studies (Birkholzer et al., 2012) showed that optimal extraction rate functions for constant injection rate cases follow a specific trend, which can be represented well by the following empirical function:

$$Q_{\text{ext}}(t)=\begin{cases} 0 & \text{if } t \le t_0 \\ Q_0 \operatorname{erfc}\left(b/\sqrt{t-t_0}\right) & \text{if } t_0 < t \le t_0+t_1 \\ Q_0 \operatorname{erfc}\left(b/\sqrt{t-t_0}\right) - \operatorname{erfc}\left(b/\sqrt{t-t_0-t}\right) & \text{if } t_0+t_1 < t \le t_2 \\ 0 & \text{if } t_2 < t \end{cases} \quad (10)$$

Applying a functional relationship for the time-dependent extraction drastically reduces the number of unknowns, if the function type is known, compared to a discrete extraction rate function that would require using many time periods with different unknown uniform rates to approximate an optimal condition. Although Eq. (10) is empirical and intuitively obtained based on our previous observations, its parameters have meanings to some extent (see Fig. 6). The time t_0 corresponds to start of the extraction right before a threshold pressure buildup value is exceeded in impact zones. The time t_1 indicates the time associated with the peak value of the extraction function, which for continuous injections usually happens immediately after the end of the injection period. At times greater than t_2, the pressure buildup falls below the threshold value without the need for further extraction.

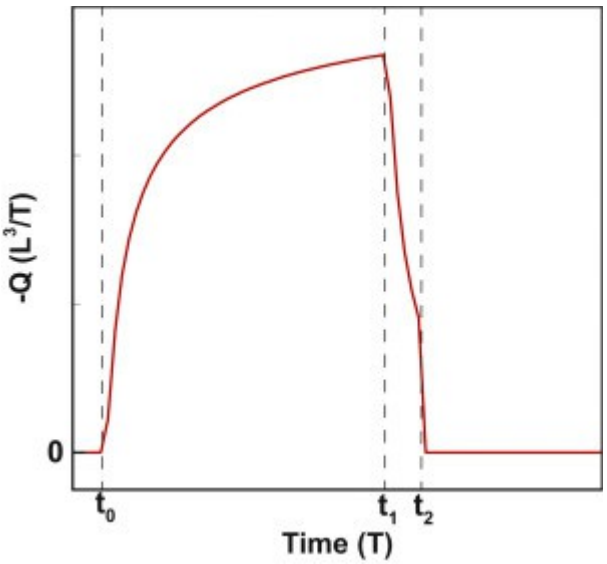

Download high-res image (108KB)

Download full-size image

Fig. 6. Schematic of the empirical extraction rate function (Eq. (10)) used in this study for the optimization calculations.

Eq. (10) contains five unknown parameters that need to be estimated for each brine extraction well. The other two unknowns are location parameters (r_i,θ_i) for each extraction well. In order to more effectively search the space for well locations, we represented the extraction well locations with respect to the distance (r_i) from the location of the injection well (x_{inj} = 295,868 m, y_{inj} = 3934,700 m) and the angle (θ_i) between the distance vector and the x-axis of the model domain. The Cartesian coordinates of the extraction wells ($x_{ext,i}$, $y_{ext,i}$) according to the frame of the numerical model domain can be expressed as $x_{ext,i} = x_{inj} + r_i\cos\theta_i$ and $y_{ext,i} = y_{inj} + r_i\sin\theta_i$.

Including the locations, the total number of unknowns for two extraction wells is equal to 14. The CDE algorithm was employed to solve the 14D optimization problems for minimizing the brine extraction ratio in each realization of the reservoir heterogeneity. We chose NP = 5 × D for all the optimization calculations in this section, and the other parameters are the same as selected in Section 3.2. The number of objective function evaluations during the five optimization runs was approximately between 8000 and 11,000.

Fig. 7 demonstrates contour plots of pressure buildup (black lines with values in MPa) and the maximum extent of the CO_2 plume (red line) at 50 years based on the optimization result of Realization 1. The figure also shows the location of the two brine extraction wells close to the faults on the east and the west sides. The CDE optimization methodology minimized the extraction ratio and successfully satisfied Constraints 1 and 2 for all the realizations (see Fig. 8b). Table 4 summarizes the optimization results for the realizations. Estimated minimum extraction ratios range from 38% to 67%. Fig. 9 shows the estimated total extraction rates (from 1 or 2 wells) as a function of time. The highest extraction ratio occurs for Realization 1 with the extraction period extending about 5 years beyond the end of injection. This is consistent with our earlier simulations without brine extraction where the lowest injection rate without threshold violation occurred for Realization 1 (Table 3).

From Fig. 7, qualitatively it can be seen that lower permeability zones around the injection zone and between the faults are more extensive relative to the other realizations. This causes stronger pressure buildup and thus requires the highest extraction ratio. Likewise, according to the contour maps of the log permeability for the generated heterogeneous fields (Fig. 10), the lowest extraction ratio occurring in Realization 3 appears to correlate with the presence of relatively high permeability zones around the faults, especially on the east side where the injected CO_2 flows mainly in that direction. In Realizations 2 and 3, a single extraction well was sufficient to achieve a minimum brine extraction ratio and to meet the constraints. The CDE algorithm gave zero production for the second extraction wells in those cases.

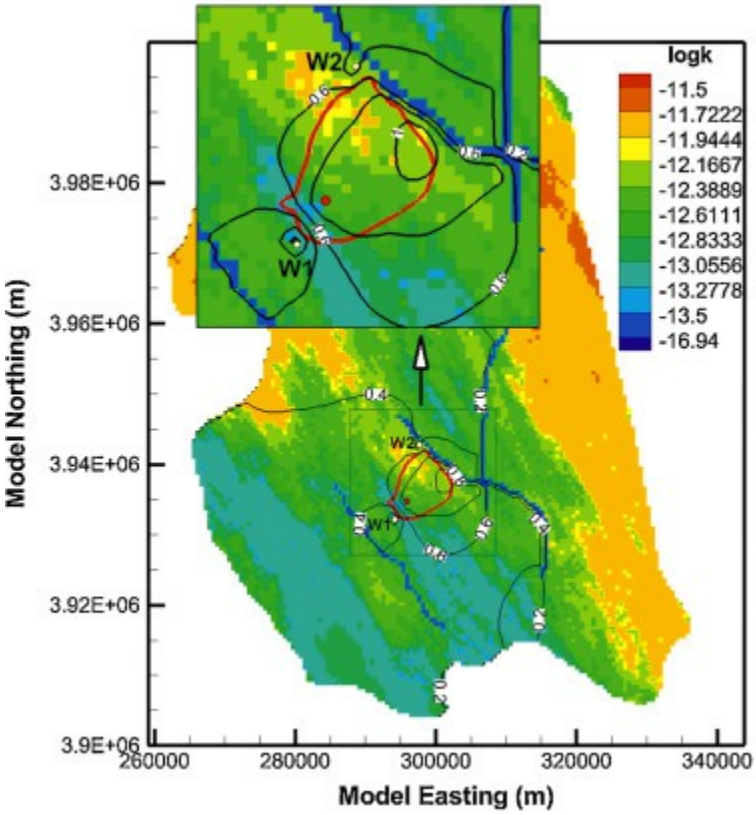

Download high-res image (557KB)

Download full-size image

Fig. 7. Optimization results for Realization 1: Pressure buildup (black contour lines with values in MPa) contour lines and CO_2 plume extent (red line, CO_2 saturation cut-off value = 0.05) with optimal well placement and brine extraction. (For interpretation of the references to color in this figure legend, the reader is referred to the web version of this article.)

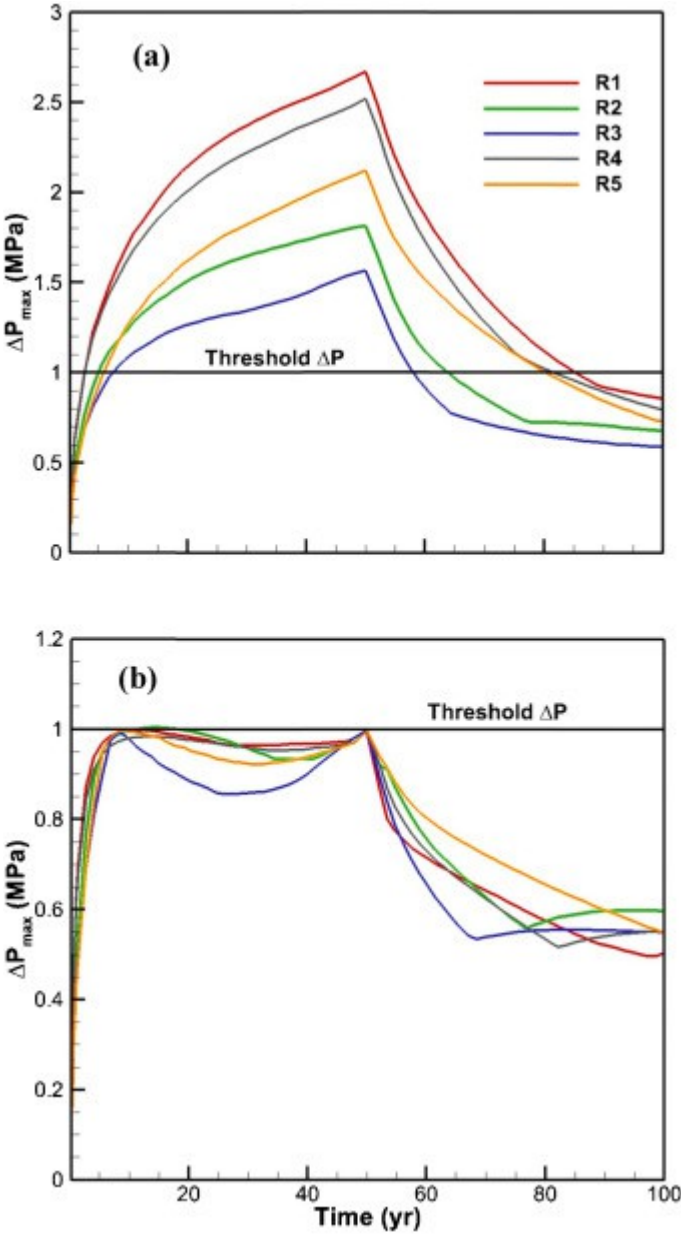

Download high-res image (379KB)

Download full-size image

Fig. 8. Evolution of maximum pressure buildup as a function of time along the three faults (a) without brine extraction and (b) with optimal brine extraction.

Table 4. Optimal parameter values of the extraction wells for 5 Mt/yr injection and ΔP_{max} = 1 MPa.

Parameters	***R*1**		***R*2**		***R*3**	***R*4**	***R*5**	
	***W*1**	***W*2**	***W*1**	***W*2**	***W*1**	***W*1**	***W*1**	***W*2**
r (km)	2.830	7.927	4.539	6.695	4.670	4.679	2.449	2.794
θ (deg)	234.927	77.485	179.304	44.233	133.569	227.825	134.704	130.368
Q_0 (m^3/s)	0.064	0.115	0.014	0.095	0.121	0.171	0.032	0.128
b^2 (yr)	0.998	0.976	0.993	0.997	0.998	0.774	0.993	0.861
t_0 (yr)	1.116	0.053	1.016	2.753	6.328	0.000	6.852	4.434

Parameters	*R*1		*R*2		*R*3	*R*4	*R*5	
	*W*1	*W*2	*W*1	*W*2	*W*1	*W*1	*W*1	*W*2
t_1 (yr)	48.000	48.338	49.290	48.058	43.112	48.002	41.752	43.792
t_2 (yr)	0.834	4.840	1.579	0.697	0. 290	0.956	0.675	1.295
Extraction ratio	0.672		0.393		0.380	0.654		0.534

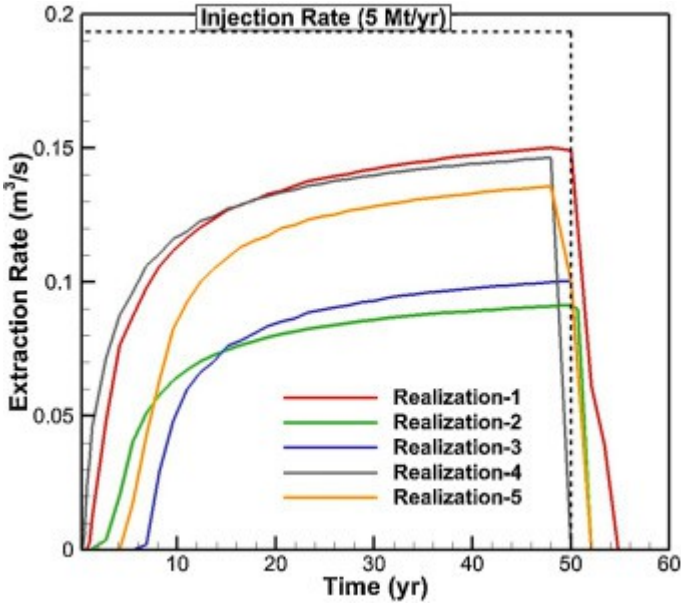

Download high-res image (277KB)

Download full-size image

Fig. 9. Total brine extraction rates through extraction wells, optimized for each realization.

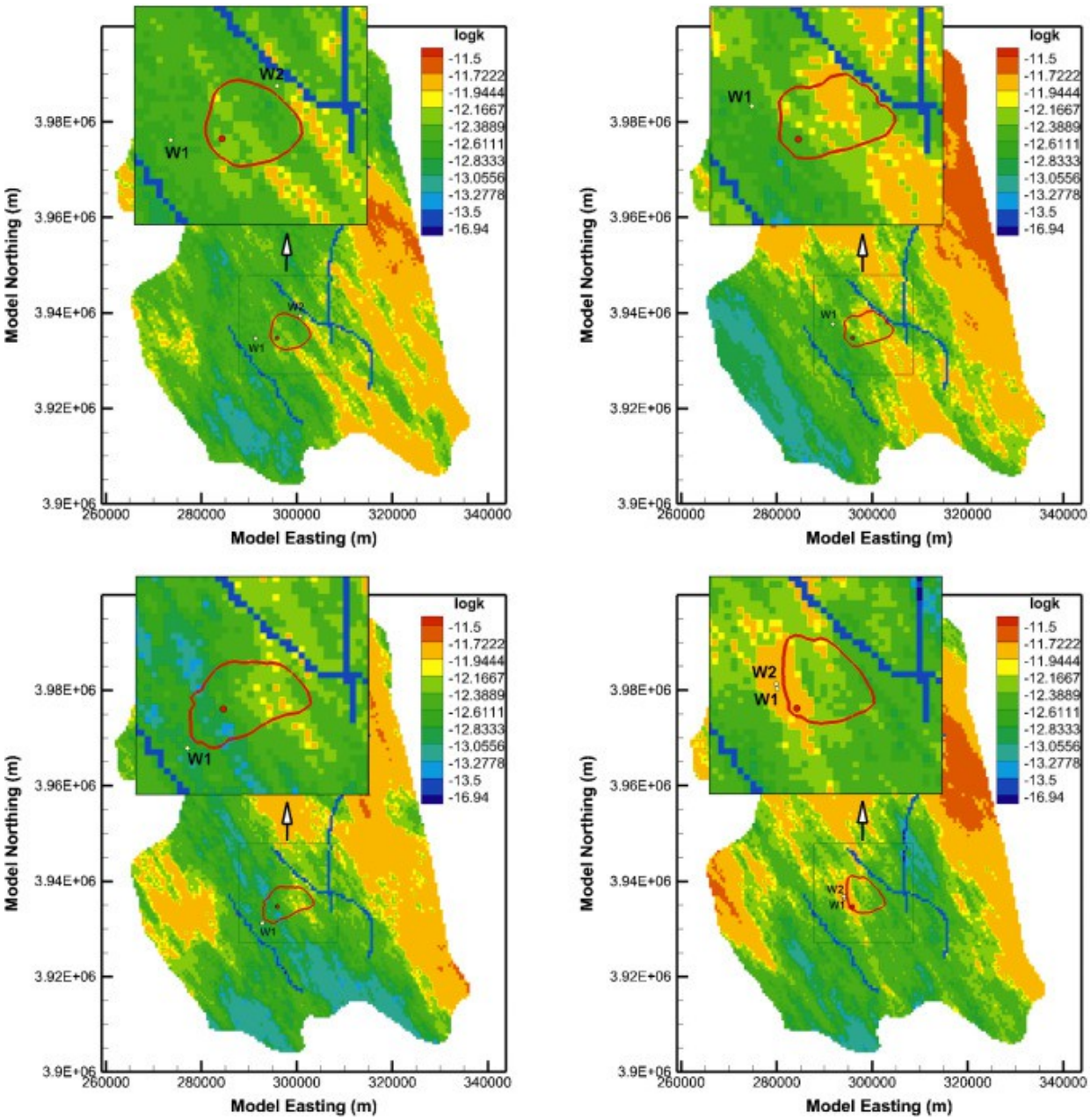

Download high-res image (2MB)

Download full-size image

Fig. 10. Optimal brine extraction well location and CO_2 plume shape (saturation cut-off value = 0.05) at the end of 50 years superimposed on the permeability (in log 10) map for realizations 2–5.

Our earlier experiences showed that under homogeneous conditions without concerns of CO_2 breakthrough in extraction wells, the minimum extraction ratios are generally achieved when the relative distance between the wells and the impact zones tend to be at minimum. However, results from this study show that heterogeneity, reservoir geometry and slope that change the CO_2 plume migration path and shape have a significant effect on the selection of well locations (Fig. 10). High variability in the extraction ratios among the different realizations (Table 4) indicates the importance of the heterogeneity and its characterization in a real CO_2 storage project. The optimum locations of the extraction wells are also affected by the heterogeneity.

5. Discussion

Optimization studies for real injection/extraction operations typically require evaluating optimal conditions for multiple realizations of hydraulic properties, especially if data are very limited and significant uncertainty exists about hydrogeological properties at the field site. The optimization methodology presented here can be utilized both during the planning stage prior to injection or at any later stage of a project. In practice, the final selection of extraction well locations and rates through optimization would wait until sufficient accurate information about local conditions and heterogeneity can be obtained from field measurements, e.g., after a few year of injection. Because forward models are iteratively updated and refined as CO_2 injection progresses and field data collection continues, the variability between different model realizations decreases as a function of time. Therefore, any decisions made based on optimization calculations at a later stage of a project will be more reliable than the decisions made before the injection starts or at an early project stage. In fact, our results in Fig. 9 show that for most realizations in this specific example brine extraction is not necessary in early injection stages because the defined pressure thresholds have not been reached. In these cases, the optimization algorithm automatically comes to the conclusion that extraction should start several years after the beginning of injection, at a time when more accurate information on the expected future pressure buildup has been obtained and the forward models have been calibrated using early time data.

By refining models and eliminating unrealistic realizations based on the data collected at high enough spatial and temporal resolutions, optimization calculations for different model realizations may be expected to result in similar estimated well locations and rates. However, because uncertainty in the reservoir model parameters can never be completely eliminated, the methodology presented in this manuscript can be applied for searching expected or average optimal conditions by simultaneously evaluating multiple reasonable realizations.

If site characterization indicates injectivity problems even before injection starts, for instance in a compartmentalized reservoir, brine extraction may need to start very early in the project. If this is the case, extraction well placement may have to be done at the beginning of the project based on the available data. Without drilling an additional well, pre-injection brine extraction may be conducted from the same injection well or another existing well, as recently suggested by Buscheck et al. (2014). If an existing well is used, the optimization problem simplifies to only estimation of well operation parameters, not well location. Whether an existing well or new well is used for extraction, forward models and optimization calculations should be updated based on continuously collected monitoring data during the project to foresee and prevent any environmental impact or to eliminate unnecessary extraction (i.e., real-time optimization).

6. Summary and conclusions

Large-scale pressure increases during GCS can potentially impact caprock integrity, induce reactivation of critically stressed faults, and drive CO_2 or brine through conductive features into shallow groundwater. Pressure management involving the extraction of native fluids from storage

formations can be used to minimize pressure increases while maximizing CO_2 storage. However, brine extraction requires pumping, transportation, possibly treatment, and disposal of substantial volumes of extracted brackish or saline water, all of which can be technically challenging and expensive. Strategic well placement and pumping can allow for a significant reduction in the total brine extraction volumes while limiting pressure increases where and when necessary.
In this study, we introduced a constrained differential evolution (CDE) algorithm for solving global optimization problems involving well placement and injection/extraction control. The CDE methodology was tested for a simple optimization problem whose solution can be partially obtained with a derivative-based optimization methodology (SQP). The CDE successfully estimated the true global optimum for both extraction well location and time-dependent extraction rates. The results from this simple test indicate the importance of selecting time-dependent extraction rates. The extraction ratio can be notably decreased by allowing the pumping rate to change as a function of time with the cost of increased number of unknown parameters.

An example application of the developed strategy was also presented for a hypothetical CO_2 storage scenario in the Vedder Formation in the Southern San Joaquin Basin in California, USA. Industrial-scale storage of CO_2 would generate significant pressure buildup in this formation, which in turn would raise concerns about induced seismicity due to presence of multiple faults surrounding the injection zone. Through the CDE optimization algorithm coupled to a numerical vertically-averaged reservoir model, we successfully estimated optimal solutions for brine extraction wells in the Vedder Formation that would result in the desired local pressure control along the faults. We also investigated how the optimized extraction rates and well locations are affected by heterogeneity in reservoir permeability and porosity.
Multiple realizations of the reservoir heterogeneity were created based on the average horizontal permeability data obtained from the existing wells in the site. In this study, we did not account for uncertainty of the reservoir properties in our optimization calculations. Rather we focused on five individual realizations to understand the impact of reservoir heterogeneity on optimization results. Our results indicate that the reservoir slope and heterogeneity have significant impact on optimum extraction rates. Reservoir heterogeneity is also a significant factor for extraction well locations, suggesting that in practice decisions about extraction well placement through optimization should be made at later project stages when data from a few years of CO_2 injection have allowed iterative updating and refining of the reservoir forward models. The highest extraction ratios appear to correlate with the presence of relatively low permeability zones around the injection well and between the faults. High variability in the extraction ratios among different permeability realizations indicates the importance of detailed site characterization and understanding of heterogeneity. Uncertainty in reservoir properties needs to be taken into account in practical applications by considering many realizations of the geological heterogeneity (e.g., Yeten et al., 2003, Wang et al., 2012).
Although our focus was on brine extraction in this work, the CDE optimization methodology presented in this paper is general enough to handle other optimization objectives related to GCS, such as reducing ‘Area of Review’, reducing risk of leakage and mitigating leakage cases, increasing storage

capacity and trapping, and for optimal monitoring design. However, further investigations are needed to determine appropriate mutation strategies and range of parameter sets used in the CDE algorithm for efficiently and accurately solving specific optimization problems. Our future work includes real-time applications of the optimization methodology for realistic CO_2storage studies in actual reservoir systems.

Acknowledgment

The authors wish to thank the two anonymous reviewers, as well as Dr. Stefan Finsterle of Lawrence Berkeley National Laboratory (LBNL), for their careful review of the manuscript and the suggestions for improvements. The work was funded by the Assistant Secretary for Fossil Energy, Office of Sequestration, Hydrogen, and Clean Coal Fuels, National Energy Technology Laboratory (NETL), of the U.S. Department of Energy under Contract No. DE-AC02-05CH11231.

References

Ahlfeld and Heidari, 1994

D.R. Ahlfeld, M. Heidari**Applications of optimal hydraulic control to ground-water systems**

ASCE J. Water Resour. Plann. Manage., 720 (3) (1994), pp. 350-365

CrossRefView Record in Scopus

Bayer and Finkel, 2004

P. Bayer, M. Finkel**Evolutionary algorithms for the optimization of advective control of contaminated aquifer zones**

Water Resour. Res., 40 (2004), p. W06506, 10.1029/2003WR002675

Bellout et al., 2012

M.C. Bellout, D.E. Ciaurri, L.J. Durlofsky, B. Foss, J. Kleppe**Joint optimization of oil well placement and controls**

Comput. Geosci. (2012), 16 (2012), pp. 1061-1079, 10.1007/s10596-012-9303-5

CrossRefView Record in Scopus

Bergmo et al., 2011

P.E. Bergmo, A. Grimstad, E. Lindeberg**Simultaneous CO_2 injection and water production to optimize aquifer storage capacity**

Int. J. Greenhouse Gas Control, 5 (2011), pp. 555-564

ArticleDownload PDFView Record in Scopus

Birkholzer et al., 2011

J.T. Birkholzer, Q. Zhou, A. Cortis, S. Finsterle**A sensitivity study on regional pressure build-up from large-scale CO_2 storage projects**

Energy Procedia, 4 (2011), pp. 4371-4378

ArticleDownload PDFView Record in Scopus

Birkholzer et al., 2012

J. Birkholzer, A. Cihan, Q. Zhou**Impact-driven pressure management via targeted brine extraction—concept studies of CO_2 storage in saline formations with leakage pathways**

Int. J. Greenhouse Gas Control, 7 (2012), p. 168

ArticleDownload PDFView Record in Scopus

Birkholzer et al., 2009

J.T. Birkholzer, Q. Zhou, C.-F. Tsang**Large-scale impact of CO_2 storage in deep saline aquifers: a sensitivity study on the pressure response in stratified systems**

Int. J. Greenhouse Gas Control, 3 (2) (2009), pp. 181-194
ArticleDownload PDFView Record in Scopus
Buscheck et al., 2011
T.A. Buscheck, Y. Sun, T.J. Wolery, W. Bourcier, A.F.B. Tompson, E.D.Jones, S.J. Friedmann, R.D. Aines**Combining brine extraction, desalination, and residual-brine reinjection with CO_2storage in saline formations: implications for pressure management, capacity, and risk mitigation. 10th International Conference on Greenhouse Gas Control Technologies, GHGT-10**
Energy Procedia, 4 (2011), pp. 4283-4290
ArticleDownload PDFView Record in Scopus
Buscheck et al., 2014
T.A. Buscheck, J.A. White, M. Chen, Y. Sun, Y. Hao, R.D. Aines, W.L.Bourcier, J.M. Bielicki**Pre-injection brine production for managing pressure in compartmentalized CO_2storage reservoirs**
Energy Procedia, 63 (2014), pp. 5333-5340
ArticleDownload PDFView Record in Scopus
Carroll et al., 2014
S.A. Carroll, E. Keating, K. Mansoor, Z. Dai, Y. Sun, W. T-Guitton, C.Brown, D. Bacon**Key factors for determining groundwater impacts due to leakage from geologic carbon sequestration reservoirs**
Int. J. Greenhouse Gas Control, 29 (2014), pp. 153-168
ArticleDownload PDFView Record in Scopus
Deng et al., 2012a
H. Deng, P.H. Stauffer, Z. Dai, Z. Jaio, R.S. Surdam**Simulation of industrial-scale CO2 storage: multi-scale heterogeneity and its impacts on storage capacity, injectivity and leakage**
Int. J. Greenhouse Gas Control, 10 (2012), pp. 397-418
ArticleDownload PDFView Record in Scopus
Cihan et al., 2011
A. Cihan, Q. Zhou, J. Birkholzer**Analytical solutions for pressure perturbation and fluid leakage through aquitards and wells in multilayered aquifer systems**
Water Resour. Res., 47 (2011), p. W10504, 10.1029/2011WR010721
Coats et al., 1971
K.H. Coats, J.R. Demsey, J.H. Henderson**The use of vertical equilibrium in two-dimensional simulation of three-dimensional reservoir performance**
Soc. Pet. Eng. J., 11 (1971), pp. 63-71
CrossRefView Record in Scopus
Court et al., 2011
B. Court, M.A. Celia, J.N. Nordbotten, T.R. Elliot**Active and integrated management of water resources throughout co_2 capture and sequestration operations. 10th International Conference on Greenhouse Gas Control Technologies, GHGT-10**
Energy Procedia 4 (2011), pp. 4221-4229
ArticleDownload PDFView Record in Scopus
Court et al., 2012
B. Court, K.W. Bandilla, M.A. Celia, A. Janzen, M. Dobossy, J.M. Nordbotten**Applicability of vertical-equilibrium and sharp-interface assumptions in CO_2sequestration modeling**
Int. J. Greenhouse Gas Control, 10 (2012), pp. 134-147

ArticleDownload PDFView Record in Scopus

Deb, 2000

K. Deb**An efficient constraint handling method for genetic algorithms**

Comput. Methods Appl. Mech. Eng., 186 (2000), pp. 311-338

ArticleDownload PDFView Record in Scopus

Deng et al., 2012b

H. Deng, P.H. Stauffer, Z. Dai, Z. Jaio, R.S. Surdam**Simulation of industrial-scale CO_2 storage: multi-scale heterogeneity and its impacts on storage capacity, injectivity and leakage**

Int. J. Greenhouse Gas Control, 10 (2012), pp. 397-418

ArticleDownload PDFView Record in Scopus

Dentz and Tartakovsky, 2009

M. Dentz, D.M. Tartakovsky**Abrupt-interface solution for carbon dioxide injection into porous media**

Transp. Porous Media, 79 (1) (2009), pp. 15-27

CrossRefView Record in Scopus

Deutsch and Journel, 1998

C.V. Deutsch, A.G. Journel**GSLIB Geostatistical Software Library and User's Guide**

(second ed.), Oxford Univ. Press, New York, NY (1998), p. 369

View Record in Scopus

Finsterle, 2004

S. Finsterle**Multiphase inverse modeling: review and iTOUGH2 applications**

Vadose Zone J., 3 (2004), pp. 747-762

CrossRefView Record in Scopus

Finsterle and Zhang, 2011

S. Finsterle, Y. Zhang**Solving iTOUGH2 simulation and optimization problems using the PEST protocol**

Environ. Modell. Softw., 26 (2011), pp. 959-968, 10.1016/j.envsoft.2011.02.008

ArticleDownload PDFView Record in Scopus

Gasda et al., 2012

S.E. Gasda, H.M. Nilsen, H.K. Dahle, W.G. Gray**Effective models for CO_2 migration in geological systems with varying topography**

Water Resour. Res., 48 (2012), p. W10546, 10.1029/2012WR012264

Gorelick, 1983

S.M. Gorelick**A review of distributed parameter groundwater management modeling methods**

Water Resour. Res., 19 (2) (1983), pp. 305-319, 10.1029/WR019i002p00305

CrossRefView Record in Scopus

Guo et al., 2014

B. Guo, K.W. Bandilla, F. Doster, E. Keilegavlen, M.A. Celia**A vertically integrated model with vertical dynamics for CO_2 storage**

Water Resour. Res., 50 (2014), 10.1002/2013WR015215

Guyagular et al., 2000

B. Guyagular, R.H. Horne, L. Rogers, J.J. Rosenzweig**Optimization of well placement in a Gulf of Mexico waterflooding project**

SPE Annual Technical Conference and Exhibition (SPE 63221), Dallas, Texas (2000)

Harto and Veil, 2011

C.B. Harto, J.A. Veil**Management of extracted water from carbon sequestration projects**
Argonne National Laboratory Report, ANL/EVS/R-11/1, January 2011 (2011), p. 38
View Record in Scopus
Harto et al., 2011
C.B. Harto, J.A. Veil, A.T. McNemar**Extracting water from carbon sequestration projects: quantities, costs, and environmental considerations**
Abstract from 10th Annual Conference on Carbon Capture & Sequestration, May 2–5, 2011, Pittsburgh, PA (2011)
Humphries et al., 2013
T.D. Humphries, R.D. Haynes, L.A. James**Simultaneous and sequential approaches to joint optimization of well placement and control**
Comput. Geosci., (2013), 10.1007/s10596-013-9375-x
Juanes et al., 2010
R. Juanes, C.W. MacMinn, M.L. Szulczewski**The footprint of the CO_2 plume during carbon dioxide storage in saline aquifers: storage efficiency for capillary trapping at the basin scale**
Transp. Porous Media, 82 (1) (2010), pp. 19-30
CrossRefView Record in Scopus
Leverett, 1941
M.C. Leverett**Capillary behaviour in porous solids**
Trans. AIME (142) (1941), pp. 159-172
Maskey et al., 2002
S. Maskey, A. Jonoski, D.P. Solomatine**Groundwater remediation strategy using global optimization algorithms**
J. Water Resour. Plann. Manage., 128 (6) (2002), pp. 431-440
CrossRefView Record in Scopus
Middleton et al., 2012
R.S. Middleton, E. Keating, P.H. Stauffer, A. Jordan, H. Viswanathan, Q.Kang, B. Carey, M. Mulkey, J. Sullivan, S.P. Chu, R. Esposito**The multiscale science of CO_2 capture and storage: from the pore scale to the regional scale**
Energy Environ. Sci., 5 (2012), p. 7328, 10.1039/C2EE03227A
CrossRefView Record in Scopus
Montoglou et al., 2004
A. Montoglou, M. Papantoniou, P. Giannoulopoulos**Management of coastal aquifers based on nonlinear optimization and evolutionary algorithms**
J. Hydrol., 297 (1–4) (2004), pp. 209-228
Nicot, 2008
J.P. Nicot**Evaluation of large-scale CO_2 storage on freshwater sections of aquifers: an example from the Texas Gulf Coast Basin**
Int. J. Greenhouse Gas Control, 2 (4) (2008), pp. 582-593
ArticleDownload PDFView Record in Scopus
Nordbotten et al., 2005
J.M. Nordbotten, M.A. Celia, S. Bachu**Injection and storage of CO_2 in deep saline aquifers: analytical solution for CO_2plume evolution during injection**
Transp. Porous Media, 58 (3) (2005), pp. 339-360
CrossRefView Record in Scopus
Parker and Lenhard, 1989

J.C. Parker, R.J. Lenhard**Vertical integration of three-phase flow equations for analysis of light hydrocarbon plume movement**
Transp. Porous Media, 5 (1989), pp. 187-206
View Record in Scopus
Pawar et al., 2014
R. Pawar, G. Bromhal, S. Carroll, S. Chu, R. Dilmore, J. Gastelum, C.Oldenburg, P. Stauffer, Y. Zhang, G. Guthrie**Quantification of key long-term risks at CO_2 sequestration sites: latest results from US DOE's National Risk Assessment Partnership (NRAP) Project**
Energy Procedia, 63 (2014), pp. 4816-4823
ArticleDownload PDFView Record in Scopus
Price et al., 2005
K. Price, R. Storn, J. Lampinen**Differential Evolution: A Practical Approach to Global Optimization**
Springer, Berlin, Germany (2005)
Rudolph, 1996
G. Rudolph**Convergence of evolutionary algorithms in general search spaces**
Proceedings of the third IEEE Conference on Evolutionary Computation, IEEE Press, New York, NY (1996), pp. 50-54
CrossRefView Record in Scopus
Sarma and Chen, 2008
P. Sarma, W.H. Chen**Efficient well placement optimization with gradient-based algorithm and adjoint models**
Proceedings of the SPE Intelligent Energy Conference and Exhibition (SPE 112257), Amsterdam, The Netherlands (2008)
Shamshiri and Jafarpour, 2012
H. Shamshiri, B. Jafarpour**Controlled CO_2 injection into heterogeneous geologic formations for improved solubility and residual trapping**
Water Resour. Res., 48 (2012), p. W02530, 10.1029/2011WR010455
Spellucci, 1998
P. Spellucci**A new technique for inconsistent problems in the SQP method**
Math. Method Oper. Res., 47 (1998), pp. 355-500
CrossRefView Record in Scopus
Storn and Price, 1996
R. Storn, K. Price**Minimizing the real functions of the ICEC'96 contest by differential evolution**
Proceedings of IEEE International Conference on Evolutionary Computation (1996), pp. 842-844
CrossRefView Record in Scopus
Storn and Price, 1997
R. Storn, K. Price**Differential evolution—a simple and efficient heuristic for global optimization over continuous spaces**
J. Global Optim., 11 (1997), pp. 341-359
CrossRefView Record in Scopus
Storn and Price, 1995
R. Storn, K.V. Price**Differential evolution: a simple and efficient adaptive scheme for global optimization over continuous spaces**
Tech. Rep. TR-95-012, Int. Comput. Sci. Instit., Berkeley, CA (1995)
Sullivan et al., 2013a

E.J. Sullivan, S.P. Chu, P.H. Stauffer, R.S. Middleton, R.J. Pawar**A method and cost model for treatment of water extracted during geologic CO_2storage**
Int. J. Greenhouse Gas Control, 12 (2013), pp. 372-381
ArticleDownload PDFView Record in Scopus
Sullivan et al., 2013b
E.J. Sullivan, S.P. Chu, P.H. Stauffer, R.J. Pawar**A CO2-PENS model of methods and costs for treatment of water extracted during geologic carbon sequestration**
Desalin. Water Treat., 51 (7–9) (2013), pp. 1487-1493
CrossRefView Record in Scopus
USGS, 2007
USGS**Petroleum systems and geologic assessment of oil and gas in the San Joaquin Basin Province**
Allegra Hosford Scheirer (Ed.), Professional Paper 1713, U.S. Geological Survey, California (2007)
Van Genuchten, 1980
M.T. Van Genuchten**A closed form equation for predicting the hydraulic conductivity of unsaturated soils**
Soil Sci. Soc. Am. J., 44 (1980), pp. 892-898
CrossRefView Record in Scopus
Wainwright et al., 2013
H. Wainwright, S. Finsterle, Q. Zhou, J.T. Birkholzer**Modeling the Performance of large-scale CO_2 storage systems: a comparison of different sensitivity analysis methods**
Int. J. Greenhouse Gas Control, 17 (2013), pp. 189-205
ArticleDownload PDFView Record in Scopus
Wang et al., 2012
H. Wang, D.E. Ciaurri, L.J. Durlofsky, A. Corminelli**Optimal well placement under uncertainty using a retrospective optimization framework**
SPE J., 5 (March (1)) (2012), pp. 112-121
CrossRefView Record in Scopus
Wu et al., 1994
Y.-S. Wu, P.S. Huyakorn, N.S. Park**A vertical equilibrium model for assessing nonaqueous phase liquid contamination and remediation of groundwater systems**
Water Resour. Res., 30 (4) (1994), pp. 903-912, 10.1029/93WR03412
CrossRefView Record in Scopus
Yeten et al., 2003
B. Yeten, L.J. Durlofksy, K. Aziz**Optimization of nonconventional well type, location, and trajectory**
SPE J., 8 (September (03)) (2003), pp. 200-210
CrossRefView Record in Scopus
Zaharie, 2002
D. Zaharie**Critical values for the control parameters of differential evolution algorithms**
R. Matoušek, P. Ošmera (Eds.), Proceedings of MENDEL 2002, 8th International Conference on Soft Computing, June 5–7, 2002, Brno University of Technology, Faculty of Mechanical Engineering, Institute of Automation and Computer Science, Brno, Brno, Czech Republic (2002), pp. 62-67
View Record in Scopus
Zandvliet et al., 2008

M.J. Zandvliet, M. Handels, G.M. van Essen, D.R. Brouwer, J.D. Jansen**Adjoint-based well-placement optimization under production constraints**
SPE J., 13 (December (04)) (2008), pp. 392-399
CrossRefView Record in Scopus
Zhang et al., 2010
K. Zhang, G. Li, A.C. Reynolds, J. Yao, L. Zhang**Optimal well placement using an adjoint gradient**
J. Pet. Sci. Eng., 73 (3–4) (2010), pp. 220-226
ArticleDownload PDFView Record in Scopus
Zhang and Agarwal, 2013
Z. Zhang, R. Agarwal**Numerical simulation and optimization of CO_2 sequestration in saline aquifers**
Comput. Fluids, 80 (2013), pp. 79-87
ArticleDownload PDFCrossRefView Record in Scopus
Zhou and Birkholzer, 2011
Q. Zhou, J.T. Birkholzer**On scale and magnitude of pressure build-up induced by large-scale geologic storage of CO_2**
Greenhouse Gases: Sci. Technol., 1 (2011), pp. 11-20, 10.1002/ghg3.001
CrossRefView Record in Scopus

[1] Present address: Environmental Modelling Department, British Geological Survey, Keyworth, Nottingham NG12 5GG, United Kingdom.